Carcinogenesis vol.0 no.0 pp.1–10, 2011
doi:10.1093/carcin/bgr303
Advance Access publication December 17, 2011

PI3K/AKT pathway regulates phosphorylation of steroid receptors, hormone independence and tumor differentiation in breast cancer

Marina Riggio, María Laura Polo, Matías Blaustein[1,2], Alejandro Colman-Lerner[1,2], Isabel Lüthy, Claudia Lanari and Virginia Novaro*

Laboratorio de Carcinogénesis Hormonal, Instituto de Biología y Medicina Experimental and [1]Instituto de Fisiología, Biología Molecular y Neurociencias, Consejo Nacional de Investigaciones Científicas y Técnicas (IBYME-CONICET), Vuelta de Obligado 2490, C1428ADN Buenos Aires, Argentina and [2]Departamento de Fisiología, Biología Molecular y Celular, Facultad de Ciencias Exactas y Naturales, Universidad de Buenos Aires, C1428EHA Buenos Aires, Argentina

*To whom correspondence should be addressed. Tel: +054 011 4783 2869; Fax: +054 011 4786 2564;
Email: vnovaro@gmail.com

Using a model of medroxyprogesterone acetate (MPA)-induced mouse mammary tumors that transit through different stages of hormone dependence, we previously reported that the activation of the phosphatidylinositol 3-kinase (PI3K)/AKT (protein kinase B) pathway is critical for the growth of hormone-independent (HI) mammary carcinomas but not for the growth of hormone-dependent (HD) mammary carcinomas. The objective of this work was to explore whether the activation of the PI3K/AKT pathway is responsible for the changes in tumor phenotype and for the transition to autonomous growth. We found that the inhibition of the PI3K/AKT/mTOR (mammalian target of rapamycin) pathway suppresses HI tumor growth. In addition, we were able to induce mammary tumors in mice in the absence of MPA by inoculating HD tumor cells expressing a constitutively active form of AKT1, myristoylated AKT1 (myrAKT1). These tumors were highly differentiated and displayed a ductal phenotype with laminin-1 and cytokeratin 8 expression patterns typical of HI tumors. Furthermore, myrAKT1 increased the tumor growth of IBH-6 and IBH-7 human breast cancer cell lines. In the estrogen-dependent IBH-7 cell line, myrAKT1 induced estrogen-independent growth accompanied by the expression of the adhesion markers focal adhesion kinase and E-cadherin. Finally, we found that cells expressing myrAKT1 exhibited increased phosphorylation of the progesterone receptor at Ser190 and Ser294 and of the estrogen receptor α at Ser118 and Ser167, independently of exogenous MPA or estrogen supply. Our results indicate that the activation of the PI3K/AKT/mTOR pathway promotes tissue architecture remodeling and the activation of steroid receptors.

Introduction

The activation of the serine–threonine protein kinase AKT/PKB (protein kinase B) is initiated when cytoplasmic AKT binds phosphatidylinositol (3,4,5)-trisphosphate at the membrane. Phosphatidylinositol (3,4,5)-trisphosphate is the product of the activity of phosphatidylinositol 3-kinase (PI3K), which is activated by different membrane receptors (1). AKT is phosphorylated by phosphatidylinositol-dependent kinase 1 at Thr308 and by the mammalian target of rapamycin complex 2 [mammalian target of rapamycin C2 (mTORC2), also known as the rictor-mTOR complex] at Ser473 (2). In cells with basal PI3K activity, AKT can also be activated by the deletion of the lipid phosphatase activity of the tumor suppressor tensin homolog (PTEN) on chromosome 10. AKT is a mediator of the protumorigenic effects of hormones and growth factors and of the anchorage-mediated survival of epithelial cells. Its activation stimulates glucose metabolism, cell cycle progression, survival and metabolism through the phosphorylation of many substrates, such as GSK3, BAX, mTOR/p70S6K, S6, TSC1 and Tpl2 (3,4).

There is increasing evidence that the PI3K/AKT signaling pathway is implicated in human breast cancer (5,6) and in resistance to endocrine (7,8), chemotherapy and radiotherapy (9,10). Consequently, inhibitors of AKT/mTOR signaling are currently being tested in clinical cancer trials (11,12). Despite increasing evidence linking mutations at the level of PI3K and PTEN with protumorigenic behavior (13,14), the direct role of AKT in cancer progression has not been genetically defined. Likewise, the contribution of AKT activation to tumorigenesis is derived from loss-of-function studies. Little is known about the tumorigenic phenotypes caused by gain-of-function mutants of AKT signaling. It has recently been shown that whereas the AKT1 isoform accelerates mammary tumor incidence, the AKT2 isoform promotes the metastasis of tumor cells without affecting the latency of tumor development (15). It is well accepted that over time, the molecular phenotypes of breast cancers can change, which impacts the design of an efficient antitumor therapy. Thus, the main goal of our study was to analyze whether the overactivation of AKT1 is directly involved in breast cancer progression and, in particular, in the acquisition of autonomous tumor growth by using two well-studied models of breast cancer.

The syngeneic experimental mouse model of mammary carcinogenesis induced by the prolonged administration of medroxyprogesterone acetate (MPA) displays all the stages of breast cancer progression, from hormone dependence to hormone independence and eventually to endocrine resistance (16). The clinical significance of the MPA-induced model lies in its similarity to the most common human breast cancers. MPA-induced mammary tumors are typically ductal adenocarcinomas, estrogen receptor (ER)- and progesterone receptor (PR)-positive and metastatic to the lung and the lymph nodes. Furthermore, we previously reported that the PI3K/AKT signaling pathway appeared to play an important role in this model of tumor progression because hormone-independent (HI) C4-HI tumors exhibited high sensitivity to anti-PI3K/AKT therapy. In contrast, hormone-dependent (HD) C4-HD tumors were more sensitive to endocrine therapy with RU-486 and ICI 182780 (17).

The human cell lines IBH-6 and IBH-7, which are derived from primary invasive ductal mammary carcinomas, are good models to study *in vivo* human breast cancer because they express steroid hormone receptors and are invasive (18). *In vivo* IBH-6 cells grow independently of the administration of 17-β-estradiol (E_2), whereas IBH-7 cells require continuous E_2 treatment to grow (19).

In the present study, we showed that the activation of the PI3K/AKT/mTOR signaling pathway was necessary and sufficient for the transition to highly differentiated and exogenous MPA- or estrogen-independent mammary tumors in a mouse model and in IBH-7 cells, respectively.

Materials and methods

Animals

Two-month-old virgin female BALB/c (IBYME Animal Facility) and nude (*nu/nu*, University of La Plata Animal Facility) mice were used. Animal care and animal procedures were approved by the Institutional guidelines in agreement with the Guide for the Care and Use of Laboratory Animals (20).

Tumors and cell lines

C4-HD is maintained by serial subcutaneous transplantation into MPA-treated BALB/c female mice. C4-HI is the HI variant of C4-HD, which arose spontaneously in an untreated mouse [reviewed in ref. (16)]. IBH-6 and IBH-7 cell lines were developed from invasive ductal breast carcinomas from two different patients (18).

Abbreviations: AKT/PKB, protein kinase B; DMEM, Dulbecco's modified Eagle's medium; ER, estrogen receptor; FAK, focal adhesion kinase; FCS, fetal calf serum; HD, hormone-dependent; HI, hormone-independent; MPA, medroxyprogesterone acetate; mTOR, mammalian target of rapamycin; PI3K, phosphatidylinositol 3-kinase; p-PTEN, phosphorylated PTEN; PR, progesterone receptor; 3D, three-dimensional.

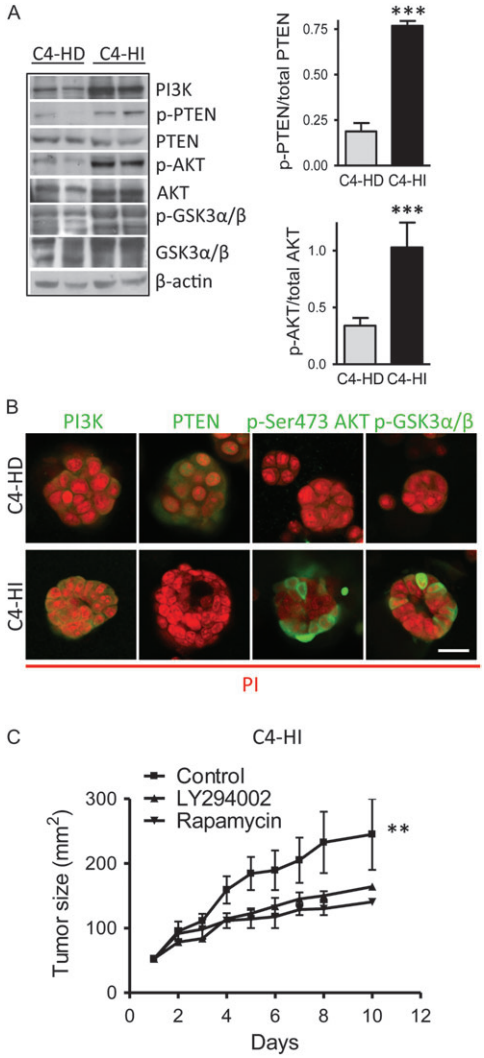

Fig. 1. Activation of the PI3K/AKT/mTOR signaling pathway is required for the growth of HI mammary tumors in mice. The C4-HI tumor cells exhibited a higher activation of the PI3K/AKT/mTOR pathway than did the C4-HD tumor cells. (**A**) Left. Western blots of protein extracts from C4-HI and C4-HD tumors growing in BALB/c females. C4-HD tumors grow in the presence of MPA. When the tumors reached 150 mm^2 in size, they were removed from the animal and processed as described in Materials and methods for western blotting. Specific antibodies against PI3K, p-PTEN, total PTEN (PTEN), AKT phosphorylated at Ser473 (p-AKT), total AKT, phosphorylated GSK3α/β (p-GSK3α/β), total GSK3α/β (GSK3α/β) and β-actin (loading control) were used. Two representative samples of a total of six of each tumor type are shown. Right, bar graphs. The quantification of PTEN inactivation (p-PTEN relative to the total PTEN levels) and AKT activation (p-AKT relative to total AKT levels). $n = 6$ for each tumor type; $^{***}P < 0.001$ (analysis of variance) C4-HI versus C4-HD. The error bars indicate the SEM. (**B**) The confocal images from immunofluorescence studies revealed that C4-HD (left) and C4-HI tumor cells (right) growing on top of Matrigel for 48 h formed cell clusters. The C4-HI cells were more organized than C4-HD cells and exhibited the presence of a central lumen in some of the clusters. The C4-HI tumor cells in 3D Matrigel preserved a higher activation of the PI3K/AKT/GSK pathway than did the C4-HD tumor cells. The PI3K, PTEN, p-Ser473 AKT and p-GSK3α/β markers were stained green with specific antibodies for immunofluorescence; the nuclei were stained red with propidium iodide. Representative clusters under each condition are shown here. Scale bar: 50 μm. (**C**) A total of 4 mg/kg of LY294002 (PI3K inhibitor), 20 mg/kg of rapamycin (mTOR inhibitor) or 100 μl of saline solution (control) was administrated intraperitoneally (i. p.) every other day for 10 days to animals exhibiting palpable C4-HI tumors. The area (length and width in square millimeter) of the mammary tumors was measured every second day using a Vernier caliper to facilitate the creation of tumor growth curves. Treatments with the inhibitors began once the tumors reached a size of ∼50 mm^2 (day 0). LY294002 and rapamycin caused the C4-HI tumors to stop growing. $n = 6$ for each group; $^{**}P < 0.01$ versus LY294002 or rapamycin.

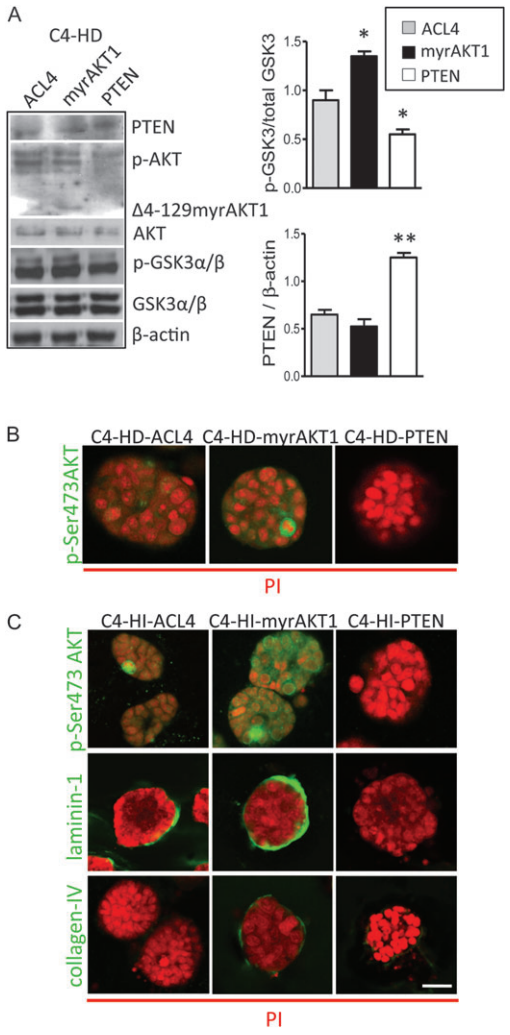

Fig. 2. Manipulation of the PI3K/AKT signaling pathway in mouse mammary tumor cells. Primary cultures derived from the C4-HD and C4-HI tumors were manipulated to display different levels of AKT activation. (**A**) Western blots from C4-HD primary cultures infected with myristoylated AKT1-Δ4-129 (myrAKT1) or wild-type PTEN (PTEN) in a retroviral vector (ACL4). Protein extracts from the infected C4-HD-PTEN tumor cells showed higher levels of total PTEN and lower levels of endogenous p-AKT than did extracts from the control C4-HD-ACL4 cells. The C4-HD-myrAKT1 tumor cells showed the expression of the endogenous phosphorylated Ser473 AKT (p-AKT) with a typical molecular weight of 59 kDa and the myristoylated deleted variant of AKT1 (p-myrΔAKT1) with a molecular weight of 45 kDa in the same gel. The antibody used to detect total AKT recognizes amino acids 71–184, which overlap with the deletion fragment in the myristoylated AKT1; for that reason, the only band observed using this antibody corresponded to the endogenous wild-type AKT. β-Actin was used as a loading control. Bottom, bar graphs. The quantification of GSK3α/β activation (p-GSK3α/β relative to total GSK3α/β levels) and PTEN induction (PTEN relative to β-actin). Phosphorylated GSK3α/β was increased in the C4-HD-myrAKT1 cells and decreased in the C4-HD-PTEN cells. PTEN was increased in the C4-HD-PTEN cells. $n = 3$ for each cell type; $^{**}P < 0.01$; $^{*}P < 0.05$ (analysis of variance) versus the C4-HD-ACL4 cells. The error bars indicate the SEM. (**B** and **C**) Confocal images from immunofluorescence studies in C4-HD (B) and C4-HI (C) cells seeded on top of Matrigel and infected with the respective constructs. The tumor cells became organized into typical clusters after 48 h. In this condition, the myrAKT1 primary cultures showed a higher intensity and number of p-Ser473 AKT-positive cells (B and C) and a more continuous deposition of the basal membrane components laminin-1 and collagen-IV (C) than did the ACL4 and PTEN primary cultures. The nuclei were stained red with propidium iodide. Representative clusters under each condition are shown. Scale bar: 50 μm.

Primary cultures

Primary cultures from C4-HD or C4-HI tumors were performed as described previously (21). Briefly, epithelial cell clusters were purified by differential sedimentation and plated in growth medium. For three-dimensional (3D) cultures, cells were seeded on top of a reconstituted basement membrane gel (Matrigel®, growth factor reduced Matrix; BD Biosciences) as described (17,22).

Culture media and drugs

Dulbecco's modified Eagle's medium (DMEM)/F12 (Sigma–Aldrich, St Louis, MO) with antibiotics (100 U/ml penicillin, 100 μg/ml streptomycin and 5 μg/ml gentamicin) were used for primary cultures. The growth medium was supplemented with 10 or 2% fetal calf serum (FCS; Natocor, Córdoba, Argentina) for either on plastic or on top of Matrigel cultures, respectively.

IBH-6 and IBH-7 cells were maintained in 10% FCS DMEM/F12 medium supplemented with 2 μg/ml bovine insulin (Invitrogen, Carlsbad, CA). When appropriate, neomycin was used to select transfected IBH-6 or IBH-7 cells. For mammosphere assay, IBH-6 cells were grown for 60 days in DMEM/F12 medium supplemented with B27 (Invitrogen), 40 ng/ml fibroblast growth factor-2 (Sigma) and 20 ng/ml epidermal growth factor (Sigma) according to Dontu *et al.* (23). LY294002 and E_2 were obtained from Sigma.

Preparation of retroviral particles for infection or transfection

Hemagglutinin epitope-tagged myristoylated human AKT1-Δ4-129 (myr-AKT1) (24) and human wild-type PTEN (25) were amplified by polymerase chain reaction and cloned into the ACL4 retroviral vector (A.C.L, unpublished, Supplementary Figure 1 is available at *Carcinogenesis* Online) consisting of a modified version of pHIT (26). Infection, selection and monitoring were done using a green fluorescent protein-G418 resistance fusion (green fluorescent protein-neomycin). Retroviral packaging was performed in HEK-293T cells using the commercial packaging system polyethylenimine (PEI87K, Pharmacy and Biochemical School, University of Buenos Aires) as per the manufacturer's instructions. Briefly, 5×10^6 HEK-293T cells were plated on 100 mm dishes with 10 ml of 10% FCS DMEM/F12 on the day prior to transfection. A 12 μg aliquot of retroviral vector, 7.5 μg of gag-pol and 4 μg of VSV G were mixed with 0.15 M NaCl to a final volume of 83 μl. The DNA was added to 750 μl of Optimem (Invitrogen) previously mixed with 35 μl of 25 mM PEI87K. The resulting solution was added to the cells and incubated at 37°C for 5 h. The medium was changed to 10 ml of fresh 10% FCS and the supernatant was removed and centrifuged at 1000*g* for 10 min 48 h post transfection. The supernatant containing the viral particles was stored at −70°C. The final titer was $>10^6$ particles/ml. For infection, exponentially growing primary cultures were mixed over 48 h with viral particles previously diluted 1:2 with fresh medium in the presence of 0.8 μg/ml polybrene (Sigma) in a six-well plate. Infected primary C4-HD and C4-HI cells were not selected. IBH-6 and IBH-7 cells were transfected with retrovirus by Lipofectamine 2000 (Invitrogen) and selected by neomycin.

In vivo *assay*

Forty-eight hours post infection of primary cultures, or confluent selected cell lines, were washed with phosphate-buffered saline 1×, detached with 0.25% trypsin, centrifuged at 1000*g* for 10 min and resuspended in a final concentration of 10^3 or 10^6 cells per 100 μl of medium for primary cultures or cell lines, respectively. The cells were subcutaneous inoculated on the right flank of nude mice. When indicated, E_2 silastic pellets (0.5 mg), which provide continuous release for over 30 days (27), were implanted subcutaneous into the back of the mice 1 week prior to cell inoculation.

Incidence of lung or lymph node metastasis (number of mice with metastasis/total number of inoculated mice) was evaluated macroscopically and microscopically after killing.

Protein extraction and western blots

Tumors were homogenized and processed to obtain total fractions for western blot as described previously (28). To prepare total protein extracts from cells, they were lysed using M-PER mammalian protein extraction reagent (Pierce, Rockford, IL). Similar amounts of protein extracts, as determined by Lowry, were loaded into each lane, and western blots were performed. The chemiluminescent substrate (ECL, Pierce) was used to detect the specific proteins in the blots.

Immunofluorescence

Cell clusters seeded on top of Matrigel in chamber slides or cell lines seeded on plastic were washed and fixed in 10% formalin for 20 min at room temperature. Fixed cells were treated with primary antibodies dissolved in blocking buffer and incubated overnight at 4°C and then with the corresponding secondary fluorescein isothiocyanate- or Texas Red-conjugated antibodies (Vector Laboratories, Burlingame, CA). Nuclei were counterstained with propidium iodide in selected experiments. Staining was analyzed under a Nikon C1 Confocal Microscope using the EZ-C1 2.20 software and a PlanApo 40X/0.95 objective.

Immunohistochemistry

Formalin-fixed paraffin-embedded tissues were reacted with the primary antibody overnight at 4°C as already described (29) and the respective secondary antibodies were accomplished by the avidin/biotin peroxidase complex technique (Vectastain Elite ABC kit; Vector Laboratories). The reactions were developed with 3-3′diaminobenzidine (Dako, Carpinteria, CA) and the nuclei were counterstained with 10% hematoxylin.

Primary antibodies

PI3K 110β, phosphorylated PTEN (p-PTEN), PTEN, p-GSK3α/β, GSK3α/β, focal adhesion kinase (FAK), ERα and β-actin all purchased from Santa Cruz Biotechnology (Santa Cruz, CA); phosphorylated Ser473 AKT, phosphorylated Ser118 ERα, phosphorylated Ser167 ERα, E-cadherin, p-S6 and S6 from Cell Signaling Technology (Danvers, MA); total AKT from BD Biosciences (Bedford, MA); p-Ser190 PR from Neomarkers, Thermo Scientific (Fremont, CA); laminin-1 from LY Laboratories (San Mateo, CA); collagen-IV from Collaborative Biomedical Products (Bedford, MA); pFAK from Invitrogen; CK14 from Covance (Emeryville, CA) and CK8 developed by Philippe Brulet and Rolf Kemler, Developmental Studies Hybridoma Bank, auspice by National Institute of Child Health and Human Development and maintained by The University of Iowa (Iowa, IA).

Statistical analysis

Western blot bands or cell staining intensities were quantified using the Image J software according to Soldati *et al.* (29) and expressed as arbitrary densitometric units. Analysis of variance and the Tukey multiple post *t*-test were used to compare means of multiple samples and the Student's *t*-test to compare the means of two different groups. Tumor growth curves were studied using regression analysis, and the slopes compared using analysis of variance followed by parallelism analysis. Data analysis was performed using the Graph Prism 4.0 software.

Results

Activation of the PI3K/AKT/mTOR signaling pathway is required for the growth of HI mammary tumors in mice

Analysis by western blot revealed that the C4-HI tumors exhibited a higher activation of PI3K, AKT and GSK3α/β compared with the C4-HD tumors (Figure 1A). AKT activation was quantified as the ratio of the AKT phosphorylated at Ser473 (p-AKT) to the total AKT (Figure 1A, bar graphs). Consistently, the fraction of the inactive form of p-PTEN also increased in the C4-HI tumors, leading to AKT activation (Figure 1A, bar graphs). The differences were not due to the presence of MPA in the C4-HD tumors because hormone treatment did not affect the higher activation of the AKT signaling pathway in the C4-HI tumors (data not shown). Immunofluorescence analysis of tumor cells grown on top of a thin laminin-rich gel (3D Matrigel; Figure 1B) showed more intense signals for PI3K, p-AKT and p-GSK3α/β, and less intense signal for PTEN, in the C4-HI than in the C4-HD cells, confirming the western blot results in the tumor samples. We previously showed (17) that C4-HI cells on Matrigel were more organized and polarized (with a central lumen in most of the clusters) than were C4-HD cells. We used 3D cultures to maintain the differences found *in vivo* between the C4-HD and C4-HI tumors in terms of PI3K/AKT/GSK3 activation because those differences are lost when these primary cells are grown on plastic (17).

We have previously suggested the involvement of the PI3K/AKT signaling pathway in C4-HI tumor growth using an inhibitor of PI3K (LY294002) (17). In the present study, we also evaluated the effects of rapamycin, an inhibitor of mTOR. Both agents decreased tumor growth similarly (Figure 1C), demonstrating that the PI3K/AKT/mTOR pathway is involved in C4-HI tumor growth.

Manipulation of the PI3K/AKT signaling pathway in mouse mammary tumor cells

To determine if the activation of the PI3K/AKT pathway *per se* is responsible for the transition to an HI tumor phenotype, we manipulated the PI3K/AKT pathway in primary tumor cultures using retroviral constructs. We used myristoylated AKT1 (myrAKT1), a constitutively active form of AKT1 with a deletion (Δ4-129 aa),

to maintain AKT1 at the cell membrane and the overexpression of PTEN to inhibit AKT activation. Each construct was cloned into the ACL4 retroviral vector (Supplementary Figure 1 is available at *Carcinogenesis* Online).

Although the efficiency of infection of the primary cultures was relatively low (~30%, as determined by green fluorescent protein-positive cells, data not shown), it was sufficient to result in changes detectable by western blot in both the C4-HD (Figure 2A) and the C4-HI (data not shown) cells. The C4-HD cells infected with PTEN showed higher levels of total PTEN and lower phosphorylation levels of endogenous AKT and its downstream effector GSK3α/β than did C4-HD cells infected with the empty vector ACL4 (Figure 2A). In contrast, the C4-HD cells infected with myrAKT1 exhibited the appropriate p-myrΔAKT1 band and an increase in p-GSK3α/β (Figure 2A).

Similar results were obtained using immunofluorescence in 3D cultures. Increased p-Ser473 AKT signals were observed in both the C4-HD-myrAKT1 (Figure 2B) and the C4-HI-myrAKT1 cultures (Figure 2C) as compared with the respective ACL4 cultures. Almost no p-Ser473 AKT staining was observed in the C4-HD-PTEN and C4-HI-PTEN cultures. As expected, the basal intensity of p-AKT and the number of positive cells were higher in the C4-HI-ACL4 than in the C4-HD-ACL4 cultures. Furthermore, the C4-HI-myrAKT1 3D cultures displayed a more continuous deposition of the basal membrane components laminin-1 and collagen-IV than did the empty vector or the PTEN cultures (Figure 2C), suggesting that the hyperactivation of AKT1 correlates with the *in vitro* basal reorganization of the basement membrane components.

Overactivation of AKT1 in mammary tumor cells leads to MPA-independent tumors in mice

To determine if the activation of the PI3K/AKT pathway also causes changes in tumor growth *in vivo*, we inoculated nude mice with C4-HD or C4-HI cells that had been previously infected with retroviral constructs expressing myrAKT1, PTEN or the empty vector ACL4.

In the absence of MPA, myrAKT1 caused the C4-HD ($P < 0.001$; Figure 3A left) and C4-HI cells ($P < 0.05$; Figure 3A right) to increase tumor growth as compared with ACL4. In contrast, PTEN inhibited C4-HI tumor growth mainly at the early time points ($P < 0.05$) without a significant effect on the C4-HD tumors. In the absence of MPA, the naive C4-HD tumor cells required >3 months post inoculation to generate tumors (data not shown), which suggested that retrovirus infection *per se* induced a protumorigenic effect, on top of which the effect of myrAKT1 was still appreciable. This effect was stronger in the C4-HD (Figure 3A and B) than in the C4-HI cells probably because the C4-HI cells already had an active PI3K/AKT pathway.

Immunohistochemical studies showed, as expected, a higher signal for p-Ser473 AKT in myrAKT1 than in the control or PTEN-expressing tumors, both in the C4-HD and in the C4-HI samples (Figure 3C and D), although the effect was less remarkable in the C4-HI tumors probably because of the high levels of endogenous p-Ser473 AKT. Nuclear and cytoplasmic staining was observed in the myrAKT1 tumors (Figure 3C and D, middle). Nuclear staining likely corresponded to endogenous AKT, which was usually observed in nuclei of uninfected cells. These results indicated that during the progression to hormone independence in this model, the activation of AKT1 constitutes a key event.

The overactivation of AKT1 in myrAKT1 tumors did not increase the incidence or size of the lung or node metastases with respect to ACL4 tumors (data not shown), suggesting that the hyperactivation of AKT1 was not involved in cell invasiveness.

To further confirm the participation of the downstream effectors of the PI3K/AKT/mTOR pathway in the determination of tumor phenotype, we evaluated PTEN levels and the phosphorylation of S6 kinase (p-S6) in C4-HD tumors. As shown in Figure 3E, PTEN was increased in the C4-HD-PTEN tumors, whereas S6 was activated in the C4-HD-myrAKT1 tumors and inhibited in the C4-HD-PTEN tumors.

MPA-independent mammary tumors originating from the overactivation of AKT1 are luminal-type and highly differentiated

To characterize the MPA-independent mammary carcinomas induced by the overactivation of AKT1, we first evaluated their histology. An increase in differentiation (the ductal-like structures indicated by black arrows in Supplementary Figure 2 is available at *Carcinogenesis* Online and Figure 4A) was observed in the C4-HD-myrAKT1 tumors compared with the C4-HD-ACL4 and C4-HD-PTEN tumors. The C4-HI-ACL4 tumors were already ductal-like and differentiated (Supplementary Figure 2 is available at *Carcinogenesis* Online), similar to the naive C4-HI tumors (17) (Figure 4B); PTEN overexpression did not change their morphology (Figure 3C and D and Supplementary Figure 2 is available at *Carcinogenesis* Online).

To further characterize these tumors, we evaluated the expression of cytokeratins 8 (CK8; luminal) and 14 (CK14; basal), as well as that of laminin-1, by immunohistochemistry. Increases in CK8 staining and in the interstitial deposition of laminin-1 were observed in the C4-HD-myrAKT1 tumors as compared with the C4-HD-ACL4 tumors, whereas no difference was observed in CK14 expression, which showed mild staining in both cases (Figure 4A). No evident alteration in CK8 or laminin-1 staining was observed in the C4-HD-PTEN tumors compared with the C4-HD-ACL4 tumors (data not shown). Interestingly, the C4-HD-myrAKT1 tumors exhibited tissue organization that was more similar to that of the naive C4-HI tumors than to that of the C4-HD tumors (Figure 4B). C4-HD-myrAKT1 and C4-HI were highly differentiated tumors, comprising abundant glandular structures surrounded by the deposition of laminin-1 and displaying high expression of CK8. These findings, consistent with the *in vitro* results shown in Figure 2D, indicated that independent of MPA supply, the overactivation of PI3K/AKT leads to the reorganization of the basement membrane and the tissue architecture in mammary tumor cells.

Overactivation of AKT1 in tumor cells results in phosphorylation of the PR

To determine the involvement of the PR in the MPA-independent tumor growth mediated by AKT1, we evaluated the phosphorylation at serine 190 (p-Ser190) of isoforms A (PRA) and B (PRB) of the PR. Both p-Ser190 PR isoforms were increased in the C4-HD-myrAKT1 tumors and reduced in the C4-HD-PTEN tumors (Figure 3E). The effect was similar in the C4-HI tumors (data not shown).

Together, these results indicate that the activation of the AKT1/mTOR pathway participates in the transition to MPA independence by activating the PR and inducing a luminal-type differentiated phenotype. This result suggests that changes in the PI3K/AKT signaling pathway could ultimately shape the response of the tumor to endocrine therapy.

Overactivation of AKT1 in human breast cancer cell lines: regulation of tumorigenicity, adhesion markers and hormone independence

To determine the mechanisms by which the overactivation of AKT1 modifies tumor behavior and to extrapolate this result to human breast cancer, we evaluated the changes in the patterns of cellular morphology and *in vivo* tumor growth of the IBH-6 and IBH-7 human breast cancer cell lines previously transfected with myrAKT1 or PTEN and selected with neomycin. IBH-6 and IBH-7 cells were grown in the presence of insulin in the growth medium and this could hyperactivate insulin and insulin-like growth factor-1 receptors; however, we still detected the effect of AKT overactivation by introducing myrAKT1. As determined by western blotting, the IBH-6-myrAKT1 cells exhibited the transfected myristoylated variant of AKT1 (p-myrΔAKT1) and increases in p-GSK3, p-S6, p-Ser167 ERα, total ERα and PRB as compared with the control IBH-6-ACL4 cells (Figure 5A). Because the PTEN levels were high in the IBH-6-ACL4 cells, the increased PTEN expression in the IBH-6-PTEN cells was not evident. Nevertheless, significant reductions in the levels of p-AKT, p-GSK3, S6, p-Ser167 ERα, total ERα and PRB were observed (Figure 5A). Neither PRA levels (Figure 5A) nor its activation (data not shown) were regulated by myrAKT1 or PTEN.

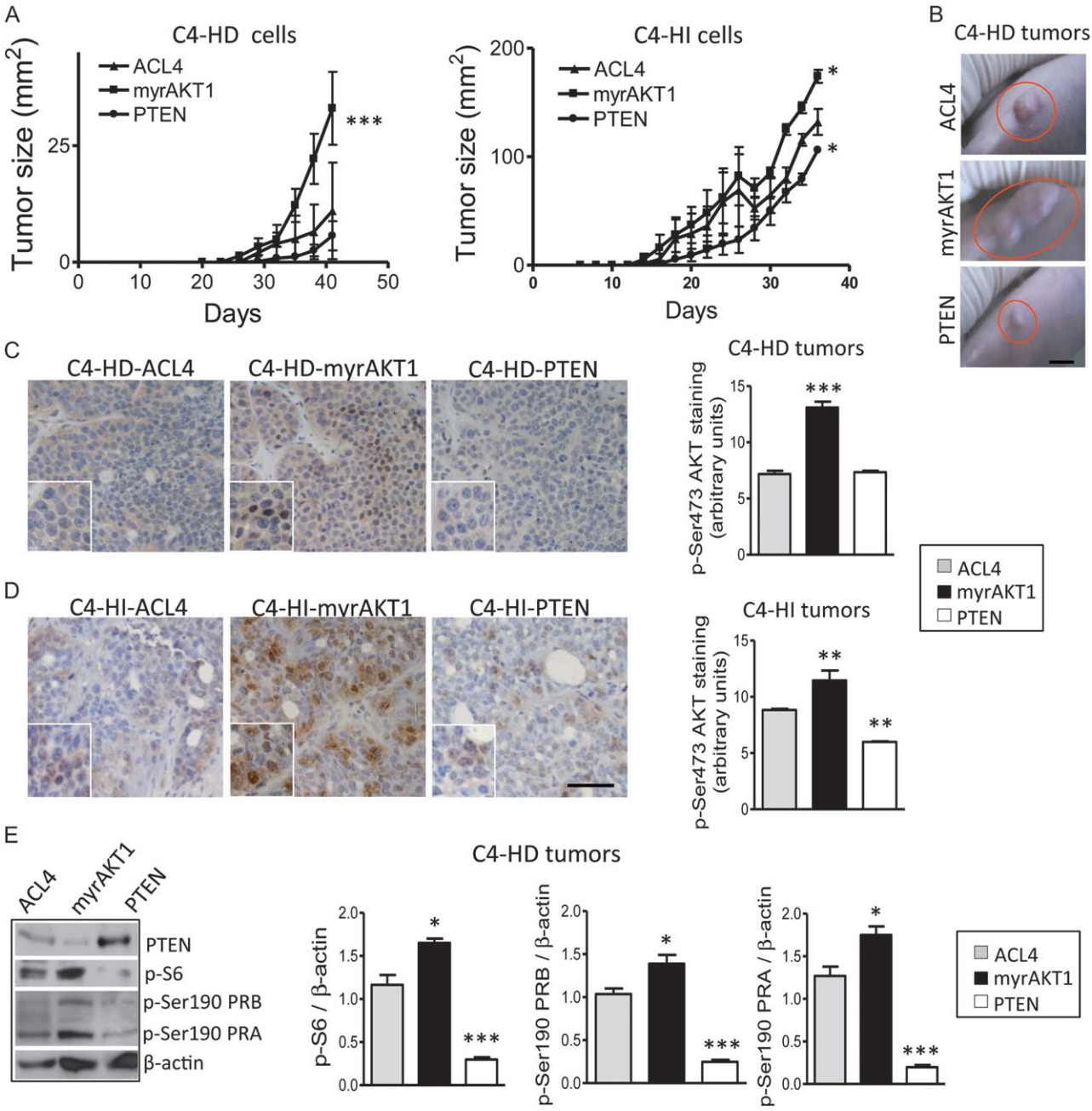

Fig. 3. Overactivation of AKT1 in mammary tumor cells leads to MPA-independent tumors in mice. Whereas the overactivation of AKT1 induced the growth of MPA-independent mammary tumor cells in nude mice, the overexpression of PTEN reduced this growth. (**A**) C4-HD (left) and C4-HI (right) tumor cells were infected with myristoylated AKT1-Δ4-129 (myrAKT1) PTEN or the control vector (ACL4), as described in Figure 2. Forty-eight hours after infection, 10^3 cells of each type were inoculated subcutaneously in the right flank of virgin nude female mice in the absence of MPA ($n = 9$). Once the tumors were palpable, after ~15 days, the length and width (square millimeter) were measured every second day, and tumor growth curves were determined for each cell type. MyrAKT1 caused the C4-HD and C4-HI cells to generate larger tumors more quickly than did the control ACL4. On the contrary, PTEN caused the C4-HI cells to generate tumors with a slower growth rate and a smaller size than those of the control cells. (**B**) Photographs of the right flanks of nude mice carrying C4-HD tumor cells infected with the three different constructs. When the tumors reached 150 mm^2 in size or ~40 days after inoculation, the animals were euthanized, and the tumor samples were removed and processed for immunohistochemistry. Scale bar: 100 mm. (**C** and **D**). Immunohistochemistry of slices of paraffin-embedded C4-HD (C) and C4-HI (D) tumors using an antibody against p-Ser473 AKT. As expected, a higher number of p-Ser473 AKT-positive cells were observed in the C4-HI tumors compared with the C4-HD control (ACL4) tumors. The number of p-Ser473 AKT-positive cells and the staining intensity increased in myrAKT1 tumors in comparison with their respective controls (ACL4), both in the C4-HD and in the C4-HI tumors, and decreased in PTEN in the C4-HI tumors. Inserts: the staining was mainly cytoplasmic in the C4-HD-ACL4 and C4-HD-PTEN tumors, although in the C4-HD-myrAKT1 tumors and all the C4-HI tumors, the nuclear staining was more evident. Brown corresponds to the antibody signal, and blue marks the nuclei that were stained with hematoxylin. Scale bar: 60 μm. The bar graphs represent a quantification of the staining intensity of p-Ser473 AKT in the C4-HD tumors (C) and the C4-HI tumors (D) in 10 fields of mammary tumors. We used Image J to quantify the staining intensity. $n = 3$ for each tumor type; $^{***}P < 0.001$; $^{**}P < 0.01$ (analysis of variance) versus the ACL4 cells. The error bars indicate the SEM. (E) Western blot of protein extracts from the C4-HD-ACL4, C4-HD-myrAKT1 and C4-HD-PTEN tumors. Specific antibodies against PTEN, phosphorylated S6 (p-S6) and phosphorylated Ser190 PR (p-Ser190 PR) were used. The last one recognized isoforms A (85 kDa) and B (115 kDa) of the receptor when phosphorylated at residue 190. Tumors derived from the C4-HD-myrAKT1 cells had lower levels of PTEN and higher levels of p-S6 and p-Ser190 PR than those derived from the control C4-HD-ACL4 cells. Tumors derived from the C4-HD-PTEN cells had higher levels of PTEN and lower levels of p-S6 and p-Ser190 PR. Right, bar graphs. The quantification of p-S6, p-Ser190 PRB and p-Ser190 PRA relative to β-actin. $n = 3$ for each cell type; $^{***}P < 0.001$; $^{*}P < 0.05$ (analysis of variance) versus the C4-HD-ACL4 cells.

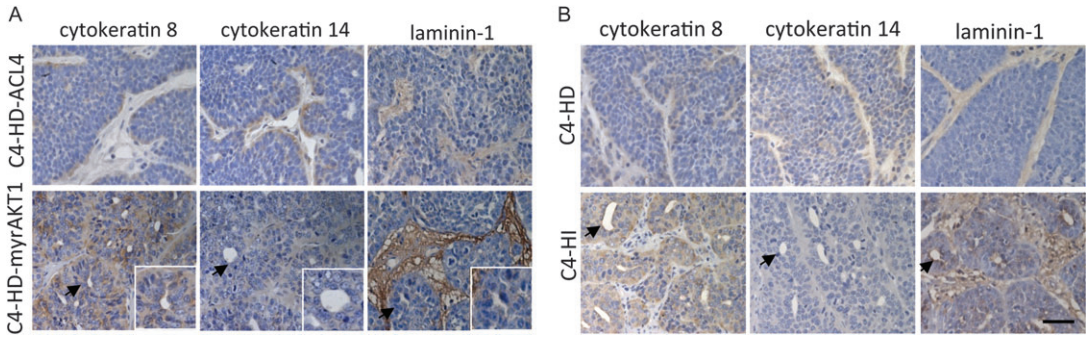

Fig. 4. MPA-independent mammary tumors originating from the overactivation of AKT1 are luminal-type and highly differentiated. Mammary tumors induced by the overactivation of AKT1 in C4-HD cells were well differentiated and were CK8- and laminin-1-positive, similar to the C4-HI mammary tumors. (**A**) Immunohistochemistry of the tumors generated in primary cells carrying distinct levels of activation of the PI3K/AKT pathway shown in Figure 3 indicated increases in CK8 (luminal marker) and interstitial laminin-1 with no significant change in CK14 (basal marker) in the C4-HD-myrAKT1 tumors compared with the C4-HD-ACL4 tumors. Histological studies corroborated the higher differentiation patterns in the C4-HD-myrAKT1 tumors compared with the C4-HD-ACL4 tumors. Ductal-like structures are indicated by black arrows and highlighted in the inserts. (**B**) The C4-HI tumors had lower CK14 and higher CK8 and laminin-1 expression than did the C4-HD tumors. Scale bar: 60 μm.

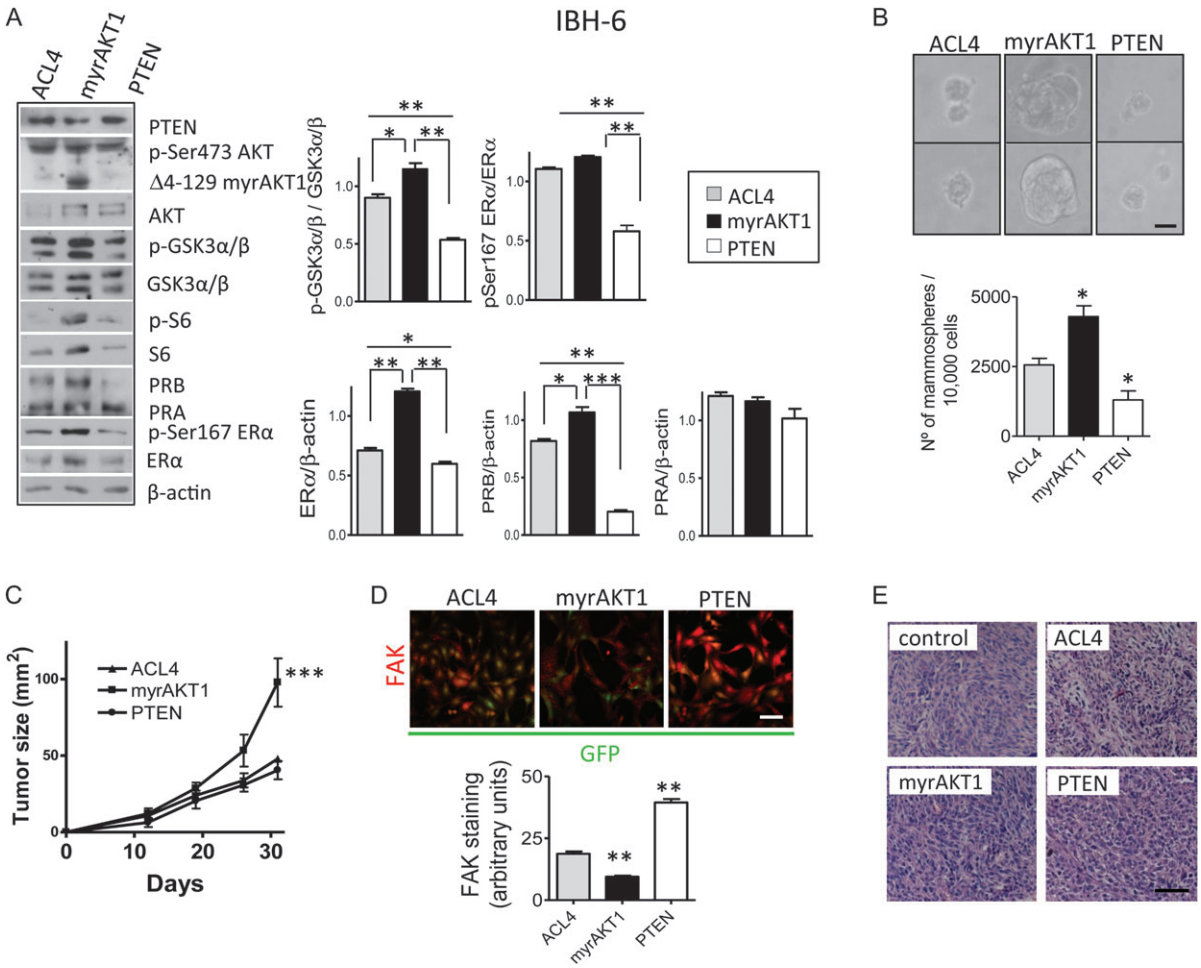

Fig. 5. Overactivation of AKT1 in IBH-6 human breast cancer cell line induces tumorigenicity *in vitro* and *in vivo*. (**A**) Estrogen-independent IBH-6 tumor cells were transfected with ACL4, myrAKT1 or PTEN and selected by neomycin. According to the western blots, the IBH-6-PTEN cells exhibited lower levels of p-AKT, p-GSK, S6, PRB and ERα than did the IBH-6-ACL4 cells. The IBH-6-myrAKT1 cells exhibited the total AKT, the endogenous p-AKT and the myristoylated deleted variant of AKT1 (p-myrΔAKT1). These cells displayed an increased in p-GSK, p-S6, Ser167 ERα, total ERα and PRB levels compared with the control IBH-6-ACL4 cells. PRA was not affected by myrAKT1 or PTEN. Right, bar graphs. The quantification of ERα, PRB and PRA relative to β-actin, p-GSK3α/β relative to total GSK3α/β and Ser167 ERα relative to ERα. $n = 3$ for each cell type; $^{***}P < 0.001$; $^{**}P < 0.01$; $^{*}P < 0.05$ (analysis of variance) versus indicated cells. (**B**) Compared with the IBH-6-ACL4 cells, the IBH-6-myrAKT1 cells formed more and bigger mammospheres, whereas the IBH-6-PTEN cells formed fewer mammospheres under the appropriate culture conditions (growth for ∼60 days in mammosphere medium, as indicated in Materials and methods). The photographs represent two different fields for each cell type under phase contrast microscopy. Scale bar: 60 μm. The bar graphs represent the number of mammospheres generated per 10 000 cells in each cell type. $n = 3$ for each cell type; $^{*}P < 0.05$ (analysis of variance) versus the IBH-6-ACL4 cells. (**C**) A total of 10^6 transfected and selected IBH-6 cells were inoculated subcutaneously into nude mice, and tumor growth curves were determined for each cell type ($n = 6$).

To evaluate if the overactivation of AKT1 induced cancer stem/progenitor cell properties, we used a mammosphere assay. In this assay, the number of mammospheres reflects the ability of self-renewal of cancer cells in an undifferentiated state, based on their ability to proliferate in suspension as non-adherent cell populations (23). In this condition, we found that the IBH-6-myrAKT1 cells formed more mammospheres than did the IBH-6-ACL4 cells (Figure 5B). The inhibition of PI3K/AKT signaling in the IBH-6-PTEN cells suppressed mammosphere formation.

To determine if an increase in the levels of AKT activation resulted in a detectable *in vivo* tumorigenic effect in estrogen-independent IBH-6 cells, we inoculated nude mice with IBH-6 cells expressing ACL4, myrAKT1 or PTEN. Tumor growth curves were determined for each cell type. The IBH-6-myrAKT1 tumors grew faster than did the control IBH-6-ACL4 or IBH-PTEN tumors ($P < 0.001$; Figure 5C). No differences were observed in tumor growth between the control cells and the IBH-PTEN cells. The incidence of tumors, ~100%, was not affected by any construct (data not shown), and the latency and slope curve (representing the pattern of tumor growth) were more similar for the ACL4 than for the naive IBH-6 cells (19). In addition, no differences in spindle cell morphology were observed between the different IBH-6-transfected cells, although the expression of the adhesion protein FAK was reduced by myrAKT1 and increased by PTEN (Figure 5D). Furthermore, no histological differences were observed between the induced tumors (Figure 5E). In summary, the overactivation of AKT1 enriched the tumorigenic progenitor cells *in vitro* and *in vivo* in IBH-6 cells, with no critical changes in cell morphology.

We then analyzed the effects of the PI3K/AKT pathway on estrogen-dependent IBH-7 cells. Surprisingly, IBH-7 cells that overexpressed PTEN did not survive more than a few days in culture. The IBH-7-myrAKT1 cells exhibited the myristoylated variant of AKT1 (p-myrΔAKT1) and increases in p-S6, p-GSK3α/β, p-Ser294 PRB, p-Ser118 ERα, p-Ser167 ERα and total ERα (Figure 6A). This last result indicated that exogenous estrogen-independent activation of ERα was mainly through an induction of ERα expression.

The overactivation of AKT was corroborated by immunofluorescence studies, in which high nuclear p-AKT staining was observed (Figure 6B). In contrast to the findings for the IBH-6 cells, the overactivation of AKT1 was associated with a change in cell morphology in the IBH-7 cells. As shown in Figure 6B, the IBH-7-myrAKT1 cells exhibited a rounded morphology. This was associated with increased levels of FAK and E-cadherin (Figure 6B). In some IBH-7-myrAKT1 cell clusters, phosphorylated FAK (p-FAK) was localized to the adhesive borders of the cells, suggesting a rudimentary polarization pattern.

We then evaluated the *in vivo* effects of the overactivation of AKT1 on IBH-7 tumorigenicity and hormone independence. We inoculated nude mice with IBH-7 cells expressing ACL4 or myrAKT1. The patterns of tumor growth (the latency and slope curve) were similar for the ACL4 cells (Figure 6C) than for the naive IBH-7 cells (19). Whereas the IBH-7-ACL4 cells required E_2 to grow, as was the case with the naïve IBH-7 cells, the IBH-7-myrAKT1 cells could surprisingly generate tumors even in the absence of E_2. However, the sizes of the IBH-7-myrAKT1 tumors were still smaller than those generated by the IBH-7-ACL4 or IBH-7-myrAKT1 cells in the E_2-treated mice. This result indicates that although gaining AKT1 function may bypass hormone dependence, other pathways that are also triggered by E_2 treatment may collaborate with AKT signaling. Finally, the incidence of lung metastasis was not affected by the expression of myrAKT1 in the IBH-7 cells (data not shown).

Together, these results indicate that the overactivation of AKT1 was sufficient to increase tumor growth and to induce a critical alteration in the cancer phenotype. Depending on the cell type, this alteration also led to changes in cell adhesion and to a conversion to ligand-independent cell growth.

Discussion

Our data show that the overactivation of AKT1 was sufficient to induce HI breast cancer growth, which suggests that upon the adaptation to hormone deprivation, breast cancer cells rely heavily on PI3K/AKT and its downstream targets mTOR, S6 and GSK3, which regulate the activation of steroid receptors and the tissue architecture of mammary carcinomas without affecting the metastatic potential of the tumor cells. Thus, our results support AKT1 as a critical driver for HI tumor growth and provide a strong rationale for the clinical use of specific PI3K/AKT/mTOR kinase inhibitors in steroid receptor-positive breast cancer. A potential candidate to initiate this activation is the tumor microenvironment because, as described previously (28), carcinoma-associated fibroblasts contribute to HI tumor growth. We postulate that under still unknown circumstances, the tumor microenvironment become 'activated' and signals to the epithelial compartment through the activation of different protein kinases, such as the PI3K/AKT pathway. Once the PI3K/AKT/GSK pathway is activated, the mechanisms of tissue remodeling and phosphorylation of steroid receptors are switched on and the tumor phenotype starts to change.

It is also interesting to note that the effects of the overactivation of AKT1 were cell line specific. Whereas the IBH-7-myrAKT1 cells underwent a notable change in cell morphology *in vitro*, no changes were observed in the IBH-6-myrAKT1 cells, indicating that even when the final result was increased tumor growth in both cell lines, the mechanisms underlying this effect may have been dependent on other signaling pathways that regulate cell proliferation. One possible explanation is that in IBH-7 cells basal levels of p-Ser473 AKT were higher than in IBH-6 cells (data not shown) suggesting that IBH-7 cells were more dependent on the PI3K/AKT pathway than IBH-6 cells.

There is extensive literature on the role of PI3K/AKT in the regulation of mammary gland differentiation at different levels (30–32). Consistent with our data showing that constitutively active AKT1 induced laminin-1 and collagen-IV deposition around C4-HD tumor cells. Li *et al.* (33) found that AKT induced the synthesis and deposition of the same proteins in differentiating C2 myoblast- and insulin-induced Chinese hamster ovary T-cell cultures. With respect to the increase in the luminal marker CK8 induced by AKT1, similar data have been reported in MCF-7 cells (34). In contrast, AKT2 has been reported to upregulate CK18 and vimentin expression in several epithelial carcinoma cell lines (35). Our data suggest that activated AKT1, as opposed to the effect of progestins (which reduce the expression of luminal cytokeratins) (36), is involved in the positive regulation of CK8 and in basement membrane formation, which are essential for epithelial cell differentiation.

We also showed that the overactivation of AKT1 increased the phosphorylation of FAK in the IBH-7 cells. FAK not only serves as a critical

MyrAKT1 caused the IBH-6 cells to grow more quickly than the control ACL4 cells. PTEN did not affect the tumor growth of the IBH-6 cells. $^{***}P < 0.001$ (analysis of variance) versus the IBH-6-ACL4 cells. (**D**) Immunofluorescence assays using Texas Red to stain for the adhesion protein FAK in IBH-6 cells in culture. FAK staining was reduced in the myrAKT1 cells and was increased in the PTEN cells. All the IBH-6 transfected cells presented a spindle-like morphology. Some nuclei of the transfected cells fluoresced green, indicating green fluorescent protein expression. Scale bar: 50 μm. The bar graphs represent a quantification of the staining intensity of FAK in 20 IBH-6 transfected cells in culture. We used Image J to quantify the staining intensity. $n = 3$ for each cell type; $^{**}P < 0.01$ (analysis of variance) versus the ACL4 cells. The error bars indicate the SEM. (**E**) All tumors that originated from the IBH-6-transfected cells were sarcomatoid and poorly differentiated, similar to the tumors that originated from the naive IBH-6 cells (control). Scale bar: 50 μm.

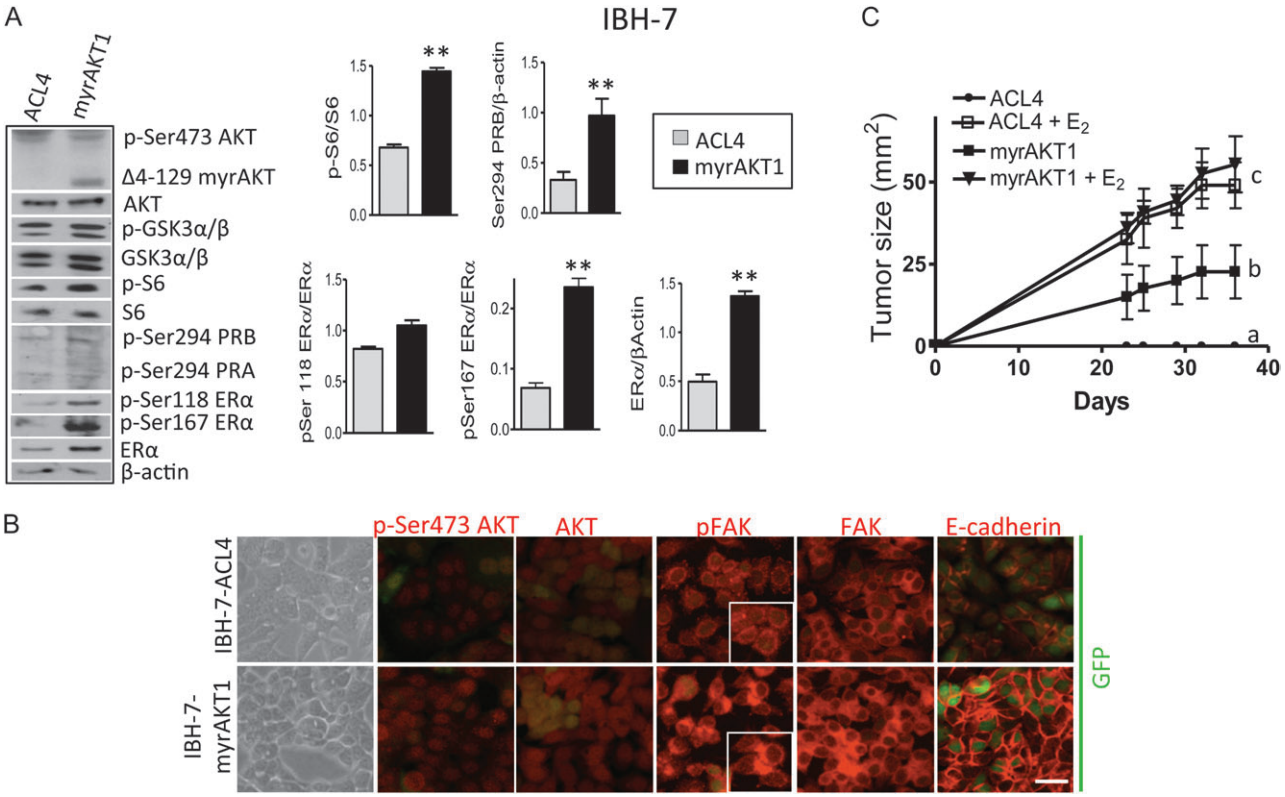

Fig. 6. Overactivation of AKT1 in IBH-7 human breast cancer cell line induces a more adhesive phenotype and an estrogen-independent tumor growth. Estrogen-dependent IBH-7 tumor cells were transfected with ACL4, myrAKT1 or PTEN and selected by neomycin. The IBH-7-PTEN cells only survived a few days in culture. (**A**) According to the western blotting results, the IBH-7-myrAKT1 cells exhibited total AKT, endogenous p-AKT and the myristoylated deleted variant of AKT1 (p-myrΔAKT1). These cells exhibited higher levels of p-S6, p-GSK3α/β, p-Ser294 PRB, p-Ser118 ERα, p-Ser167 ERα and total ERα than did the IBH-7-ACL4 cells. The bar graphs displayed the quantification of p-S6 relative to S6, p-Ser294 PRB and ERα relative to β-actin and p-Ser118 ERα and p-Ser167 ERα relative to total ERα. $n = 3$ for each cell type; $^{**}P < 0.01$ (analysis of variance) versus the IBH-7-ACL4 cells. (**B**) Top. Photographs of the IBH-7-ACL4 and IBH-7-myrAKT1 cells in culture. The IBH-7-ACL4 cells exhibited the typical polygonal shape morphology, whereas the IBH-7-myrAKT1 cells exhibited a more rounded morphology. Immunofluorescence assays using Texas Red to stain for p-Ser473 AKT, total AKT, the adhesion proteins FAK and E-cadherin in IBH-7 cells in culture. Some nuclei of transfected cells fluoresced green for green fluorescent protein. IBH-7-myrAKT1 cells displayed increased staining for p-Ser473 AKT, AKT, p-FAK, FAK and E-cadherin. In some IBH-7-myrAKT1 cell clusters, p-FAK was localized to the adhesive border of the cells. Scale bar: 25 μm. (**C**) A total of 10^6 transfected and selected IBH-7 cells expressing ACL4 or myrAKT1 were inoculated subcutaneously into nude mice, and tumor growth curves were determined for each cell type ($n = 6$). MyrAKT1 caused the IBH-7 cells to grow more quickly than the control ACL4 cells. To grow IBH-7-ACL4 cells *in vivo*, the cells were mixed with 100 μl of Matrigel and a subcutaneous pellet of 0.5 mg E_2 was administrated 1 week before cell inoculation when indicated ($+E_2$). The IBH-7-myrAKT1 cells generated tumors in the absence of the E_2 pellet. Different letters indicate significant differences between cell types with a versus b: $P < 0.05$; a versus c: $P < 0.001$; b versus c: $P < 0.01$ (analysis of variance).

component of integrin signaling but is also required for cell spreading, polarity and chemotactic invasion. Although FAK is typically considered to be upstream of AKT, it has been reported that extracellular pressure stimulates cancer cell adhesion and tumor differentiation via AKT-dependent FAK phosphorylation, suggesting a positive regulatory loop between FAK and AKT (37). Most studies have considered E-cadherin as a tumor suppressor gene, and the decreased expression of this protein has been associated with tumor progression. Moreover, AKT has been shown to repress the expression of E-cadherin in several human tumor cell lines (38). However, our results show that the overactivation of AKT1 increased E-cadherin expression in IBH-7 cells without affecting the invasive behavior of those cells.

We hypothesize that most of the effects described here for AKT1 in C4-HD and IBH-7 cells are related to the transition to a HI stage of growth. However, the same effects are not necessarily expected during the conversion to a more invasive phenotype or to increased cell proliferation in all tumor models. Consistent with this theory, we found intriguingly that in estrogen-independent IBH-6 cells, AKT1 downregulated FAK expression and upregulated the ability of these cells to form mammospheres.

Along the same lines, Blanco-Aparicio *et al.* (39) demonstrated that myrAKT1 expression in the mammary glands of transgenic mice increased the susceptibility to the induction of ER-positive mammary adenocarcinomas by 9,10-dimethyl-1,2-benzanthracene. The authors found that whereas 9,10-dimethyl-1,2-benzanthracene-treated wild-type mice exhibited mostly sarcomatous mammary tumors, AKT transgenic mice treated with 9,10-dimethyl-1,2-benzanthracene primarily developed adenocarcinomas. Similarly, others have found that female mice coexpressing activated AKT1 and ErbB-2 developed mammary tumors faster than did the activated ErbB-2 strain alone (40). Furthermore, bitransgenic mice exhibited lower levels of invasiveness, fewer metastatic lesions and more differentiated phenotypes. Hutchinson *et al.* (40) concluded that the overexpression of AKT by itself was unable to induce mammary tumors; rather, it needed another oncogenic event that would eventually synergize with the overexpression of AKT. Our findings are consistent with the hypothesis that AKT1 participates in cancer progression. In C4-HD and IBH-7 cells, the AKT1 pathway replaced the need for an exogenous hormone supply by inducing morphological cell changes that may have exploited ligand-independent hormone receptor pathways. However, in IBH-6 cells that already grew without a hormone supply, the mechanism related to increased tumor growth may have been different, favoring the expansion of subpopulations with stem cell-like properties. The role of the AKT/GSK3 pathway in enriching the mammary cancer stem/progenitor cell compartment has been demonstrated *in vitro* and *in vivo* by others (41).

Our results showed that the overactivation of AKT1 led to exogenous MPA- or estrogen-independent activation of the PR and ERα through an increase in the total expression level of the steroid receptors. These findings are promising because there is extensive literature regarding the regulation of the phosphorylation of ER by AKT and ERK (42–44). According to http://www.hprd.org/PhosphoMotif_finder, Ser167 of ERα is a consensus phosphorylation site for AKT and other seven kinases; thus, it might be a direct target of AKT in IBH-6 and IBH-7 cells. Ser118 of ERα is a known consensus phosphorylation site for ERK and it could be a target of other three kinases, GSK3 among them. On the other hand, little is known about the regulation of the phosphorylation of PR (45) or steroid receptors expression (17) by protein kinases. Miller *et al.* (46) showed that PTEN loss, which overactivates AKT, reduced ER, PRA and PRB expression but increased transcriptional activity of ER in MCF-7 cells. However, in T47D cells, PTEN loss reduced both expression and transcriptional activity of ER and PR. Such findings, even contrary to our results, support the idea that the final effect of the overactivation of the PI3K/AKT pathway is cell line specific. Thus, ligand-independent activation of ER or PR through kinase activity deregulation may underlie the mechanisms that contribute to acquired HI growth and, ultimately, endocrine resistance.

Miller *et al.* (47) demonstrated that PI3K and mTOR inhibition prevented the emergence of hormone-resistant breast cancer cells, suggesting that PI3K is required for the adaptation of ER-positive cells to hormone deprivation. Our findings suggest that acquired autonomous growth may be abrogated by combination therapies targeting both steroid receptors and protein kinases. Preclinical trials in animal models of breast tumor progression, such as those used here, will be critical in the design of better therapies targeting PI3K/AKT/mTOR for the maximal prevention of HI cell growth. Furthermore, early intervention with combined endocrine and PI3K-directed therapies could limit the resistance to antiestrogens and antiprogestins in ER/PR-positive mammary tumors and could ultimately circumvent the occurrence of endocrine resistance when the remaining tumor cells switch to a complementary intracellular signal.

Supplementary material

Supplementary and Figures 1 and 2 can be found at http://carcin.oxfordjournals.org/.

Funding

Sciences and Technology Secretary (SECyT) (PICT 07 00939); National Council for Scientific and Technical Research (CONICET) (PIP 2010–2012 N° 692); SALES Foundation Argentina. The funders had no role in study design, data collection and analysis, decision to publish or preparation of the manuscript.

Acknowledgements

We are very grateful to Pablo Do Campo and Bruno Luna for excellent technical assistance. We also thank Dr Richard Roth (Stanford School of Medicine, CA) for kindly provided myristoylated AKT1 plasmid; to Dr Keith Yamada (NIH, Bethesda, MD) for PTEN plasmid; to Laboratorios Craveri, Argentina for MPA and to Dr Silvio Gutkind (NIDCR/NIH) for sharing selected reagents.

Conflict of Interest Statement: None declared.

References

1. Feng,J. *et al*. (2004) Identification of a PKB/Akt hydrophobic motif Ser-473 kinase as DNA-dependent protein kinase. *J. Biol. Chem.*, **279**, 41189–41196.
2. Sarbassov,D.D. *et al*. (2005) Phosphorylation and regulation of Akt/PKB by the rictor-mTOR complex. *Science*, **307**, 1098–1101.
3. Carracedo,A. *et al*. (2008) The PTEN-PI3K pathway: of feedbacks and cross-talks. *Oncogene*, **27**, 5527–5541.
4. Wickenden,J.A. *et al*. (2010) Key signalling nodes in mammary gland development and cancer. Signalling downstream of PI3 kinase in mammary epithelium: a play in 3 Akts. *Breast Cancer Res.*, **12**, 202
5. Perez-Tenorio,G. *et al*. (2002) Activation of AKT/PKB in breast cancer predicts a worse outcome among endocrine treated patients. *Br. J. Cancer*, **86**, 540–545.
6. Wu,Y. *et al*. (2008) Clinical significance of Akt and HER2/neu overexpression in African-American and Latina women with breast cancer. *Breast Cancer Res.*, **10**, R3
7. Tokunaga,E. *et al*. (2006) The association between Akt activation and resistance to hormone therapy in metastatic breast cancer. *Eur. J. Cancer*, **42**, 629–635.
8. Beeram,M. *et al*. (2007) Akt-induced endocrine therapy resistance is reversed by inhibition of mTOR signaling. *Ann. Oncol.*, **18**, 1323–1328.
9. Knuefermann,C. *et al*. (2003) HER2/PI-3K/Akt activation leads to a multidrug resistance in human breast adenocarcinoma cells. *Oncogene*, **22**, 3205–3212.
10. Stal,O. *et al*. (2003) Akt kinases in breast cancer and the results of adjuvant therapy. *Breast Cancer Res.*, **5**, R37–R44.
11. Di Cosimo,S. *et al*. (2008) Targeted therapies in breast cancer: where are we now? *Eur. J. Cancer*, **44**, 2781–2790.
12. Alvarez,R.H. *et al*. (2010) Emerging targeted therapies for breast cancer. *J. Clin. Oncol.*, **28**, 3366–3379.
13. Tokunaga,E. *et al*. (2007) Coexistence of the loss of heterozygosity at the PTEN locus and HER2 overexpression enhances the Akt activity thus leading to a negative progesterone receptor expression in breast carcinoma. *Breast Cancer Res. Treat.*, **101**, 249–257.
14. Mills,G.B. *et al*. (2001) The role of genetic abnormalities of PTEN and the phosphatidylinositol 3-kinase pathway in breast and ovarian tumorigenesis, prognosis, and therapy. *Semin. Oncol.*, **28**, 125–141.
15. Dillon,R.L. *et al*. (2010) Distinct biological roles for the akt family in mammary tumor progression. *Cancer Res.*, **70**, 4260–4264.
16. Lanari,C. *et al*. (2009) The MPA mouse breast cancer model: evidence for a role of progesterone receptors in breast cancer. *Endocr. Relat. Cancer*, **16**, 333–350.
17. Polo,M.L. *et al*. (2010) Responsiveness to PI3K and MEK inhibitors in breast cancer. Use of a 3D culture system to study pathways related to hormone independence in mice. *PLoS One*, **5**, e10786
18. Vazquez,S.M. *et al*. (2004) Three novel hormone-responsive cell lines derived from primary human breast carcinomas: functional characterization. *J. Cell. Physiol.*, **199**, 460–469.
19. Bruzzone,A. *et al*. (2009) Novel human breast cancer cell lines IBH-4, IBH-6, and IBH-7 growing in nude mice. *J. Cell. Physiol.*, **219**, 477–484.
20. Institute of Laboratory Animal Resources, C.o.L.S.N.R.C. (1996) *Guide for the Care and Use of Laboratory Animals*. National Academy Press, Washington, DC
21. Lanari,C. *et al*. (2001) Five novel hormone-responsive cell lines derived from murine mammary ductal carcinomas: in vivo and *in vitro* effects of estrogens and progestins. *Cancer Res.*, **61**, 293–302.
22. Lee,G.Y. *et al*. (2007) Three-dimensional culture models of normal and malignant breast epithelial cells. *Nat. Methods*, **4**, 359–365.
23. Dontu,G. *et al*. (2003) *In vitro* propagation and transcriptional profiling of human mammary stem/progenitor cells. *Genes Dev.*, **17**, 1253–1270.
24. Kohn,A.D. *et al*. (1996) Akt, a pleckstrin homology domain containing kinase, is activated primarily by phosphorylation. *J. Biol. Chem.*, **271**, 21920–21926.
25. Tamura,M. *et al*. (1998) Inhibition of cell migration, spreading, and focal adhesions by tumor suppressor PTEN. *Science*, **280**, 1614–1617.
26. Soneoka,Y. *et al*. (1995) A transient three-plasmid expression system for the production of high titer retroviral vectors. *Nucleic Acids Res.*, **23**, 628–633.
27. Kordon,E. *et al*. (1990) Hormone dependence of a mouse mammary tumor line induced *in vivo* by medroxyprogesterone acetate. *Breast Cancer Res. Treat.*, **17**, 33–43.
28. Giulianelli,S. *et al*. (2008) Carcinoma-associated fibroblasts activate progesterone receptors and induce hormone independent mammary tumor growth: a role for the FGF-2/FGFR-2 axis. *Int. J. Cancer*, **123**, 2518–2531.
29. Soldati,R. *et al*. (2009) Inhibition of mammary tumor growth by estrogens: is there a specific role for estrogen receptors alpha and beta? *Breast Cancer Res. Treat.*, **123**, 709–724.
30. Li,G. *et al*. (2002) Conditional loss of PTEN leads to precocious development and neoplasia in the mammary gland. *Development*, **129**, 4159–4170.

31. Irie,H.Y. *et al*. (2005) Distinct roles of Akt1 and Akt2 in regulating cell migration and epithelial-mesenchymal transition. *J. Cell Biol.*, **171**, 1023–1034.
32. Maroulakou,I.G. *et al*. (2008) Distinct roles of the three Akt isoforms in lactogenic differentiation and involution. *J. Cell. Physiol.*, **217**, 468–477.
33. Li,X. *et al*. (2001) Akt/PKB regulates laminin and collagen IV isotypes of the basement membrane. *Proc. Natl Acad. Sci. USA*, **98**, 14416–14421.
34. Vandermoere,F. *et al*. (2007) Proteomics exploration reveals that actin is a signaling target of the kinase Akt. *Mol. Cell. Proteomics*, **6**, 114–124.
35. Fortier,A.M. *et al*. (2010) Akt isoforms regulate intermediate filament protein levels in epithelial carcinoma cells. *FEBS Lett.*, **584**, 984–988.
36. Sartorius,C.A. *et al*. (2005) Progestins initiate a luminal to myoepithelial switch in estrogen-dependent human breast tumors without altering growth. *Cancer Res.*, **65**, 9779–9788.
37. Wang,S. *et al*. (2011) Akt directly regulates focal adhesion kinase through association and serine phosphorylation: implication for pressure-induced colon cancer metastasis. *Am. J. Physiol. Cell Physiol.*, **300**, C657–C670.
38. Julien,S. *et al*. (2007) Activation of NF-kappaB by Akt upregulates Snail expression and induces epithelium mesenchyme transition. *Oncogene*, **26**, 7445–7456.
39. Blanco-Aparicio,C. *et al*. (2007) Mice expressing myrAKT1 in the mammary gland develop carcinogen-induced ER-positive mammary tumors that mimic human breast cancer. *Carcinogenesis*, **28**, 584–594.
40. Hutchinson,J.N. *et al*. (2004) Activation of Akt-1 (PKB-alpha) can accelerate ErbB-2-mediated mammary tumorigenesis but suppresses tumor invasion. *Cancer Res.*, **64**, 3171–3178.
41. Korkaya,H. *et al*. (2009) Regulation of mammary stem/progenitor cells by PTEN/Akt/beta-catenin signaling. *PLoS Biol.*, **7**, e1000121
42. Campbell,R.A. *et al*. (2001) Phosphatidylinositol 3-kinase/AKT-mediated activation of estrogen receptor alpha: a new model for anti-estrogen resistance. *J. Biol. Chem.*, **276**, 9817–9824.
43. Sun,M. *et al*. (2001) Phosphatidylinositol-3-OH Kinase (PI3K)/AKT2, activated in breast cancer, regulates and is induced by estrogen receptor alpha (ERalpha) via interaction between ERalpha and PI3K. *Cancer Res.*, **61**, 5985–5991.
44. Massarweh,S. *et al*. (2008) Tamoxifen resistance in breast tumors is driven by growth factor receptor signaling with repression of classic estrogen receptor genomic function. *Cancer Res.*, **68**, 826–833.
45. Vicent,G.P. *et al*. (2006) Chromatin remodeling and control of cell proliferation by progestins via cross talk of progesterone receptor with the estrogen receptors and kinase signaling pathways. *Ann. N. Y. Acad. Sci.*, **1089**, 59–72.
46. Miller,T.W. *et al*. (2009) Loss of phosphatase and tensin homologue deleted on chromosome 10 engages ErbB3 and insulin-like growth factor-I receptor signaling to promote antiestrogen resistance in breast cancer. *Cancer Res.*, **69**, 4192–4201.
47. Miller,T.W. *et al*. (2010) Hyperactivation of phosphatidylinositol-3 kinase promotes escape from hormone dependence in estrogen receptor-positive human breast cancer. *J. Clin. Invest.*, **120**, 2406–2413.

Received August 25, 2011; revised December 3, 2011; accepted December 11, 2011